Original Article

Examining the Phytochemical Analysis, In Vitro Cytotoxicity, and Antimicrobial Effects of Rotundine Glycoside Isolated From *Cyperus rotundus* L. Rhizomes

Mohammed N Sabir[1], Selar Izzat[2], Shahlaa M Abdullah[3], Bahez O Ismael[4], Kawkab Y Saour[5], Shwan Rachid[6*]

1. Department of Pharmacognosy and Pharmaceutical Chemistry, College of Pharmacy, University of Sulaimani, Sulaymaniyah, Iraq.
2. Department of Biology, College of Science, University of Sulaimani, Sulaymaniyah, Iraq.
3. Department of Medical Laboratory Science, College of Science, University of Raparin, Ranya, Iraq.
4. Kurdistan Institution for Strategic Studies and Scientific Research, Sulaymaniyah, Iraq.
5. Department of Pharmaceutical Chemistry, College of Pharmacy, University of Baghdad, Baghdad, Iraq.
6. Charmo Center for Research and Training, Charmo University, Chamchamal, Iraq.

*** Corresponding Author:**
Shwan Rachid, Professor.
Address: Charmo Center for Research and Training, Charmo University, Chamchamal, Iraq.
Phone: +96 (477) 01494344
E-mail: shwan.rachid@charmouniversity.org

Article info:
Received: 12Jun 2023
Accepted: 15 Jul 2023

Keywords:
Alkaloids, Antimicrobial, Chromatography, *Cyperus rotundus*, Anticancer, Natural products

ABSTRACT

Background: Plant metabolites, like antimicrobial and cytotoxic effects, exhibit therapeutic benefits. The crude extract of *Cyperus rotundus* (CR) rhizomes demonstrates such activities; however, the specific components responsible for these functions have not been determined.
Objectives: This study identifies the bioactive alkaloids in CR rhizome extract.

Methods: The crude methanolic extract of CR rhizomes was acidified, followed by basification. The precipitate was then purified using sequential chromatographic and high-performance liquid chromatography techniques. Structural elucidation of the derived compound was performed using the Fourier-transform infrared spectroscopy, proton nuclear magnetic resonance, and mass spectroscopy. Disc dilution and diffusion assays were used to evaluate the isolated compound's minimum inhibitory concentrations (MICs) and minimum bactericidal concentrations (MBCs) against selected microbial species. The cytotoxicity of the isolated compound was determined against HeLa cancer cells using MTT cell proliferation assays.

Results: Spectral analysis confirmed the presence of norrotundine-6-O-glucoside plus appreciable amounts of flavonoids nootkatone, quercetin, chlorogenic acid, catechin, and β-sitosterol. The isolated alkaloid inhibited the growth of *Staphylococcus aureus* (MIC=MBC=64 µg/mL), *Escherichia coli* (MIC=100 µg/mL), and *Candida albicans* (MIC=MBC=64 µg/mL). The alkaloid's half-maximal inhibitory concentration (IC_{50}) was 203.7 µg/mL. The obtained alkaloid from the CR rhizomes' crude extract revealed bactericidal and fungicidal effects against *S. aureus* and *C. albicans*, respectively, at 64 µg/mL, bacteriostatic against *E. coli* at 100 µg/mL, and cytotoxic against HeLa cells at an IC_{50} equal to 203.7 µg/mL.

Conclusion: The elucidated alkaloid from the CR rhizomes' crude extract exhibited bactericidal and fungicidal effects against *S. aureus* and *C. albicans*, respectively, at 64 µg/mL, bacteriostatic activity against *E. coli* at 100 µg/mL and cytotoxicity against HeLa cells at IC_{50} of 203.7 µg/mL.

Citation Sabir MN, Izzat S, Abdullah SM, Ismael BO, Saour KY, Rachid S. Examining the Phytochemical Analysis, In Vitro Cytotoxicity, and Antimicrobial Effects of Rotundine Glycoside Isolated From *Cyperus rotundus* L. Rhizomes. Pharmaceutical and Biomedical Research. 2024; 10(1):57-72. http://dx.doi.org/10.32598/PBR.10.1.1234.1

http://dx.doi.org/10.32598/PBR.10.1.1234.1

PBR
Pharmaceutical & Biomedical Research

Introduction

The dramatic demand to locate potential new molecules in anticancer and antimicrobials is associated with increased resistant microbial strains and cancer cells against the existing medications. Screening nature was and still is one of the valuable resources in this field because of its ability to accommodate various external changes. Among the natural sources, herbs with previous records of medicinal benefits are considered an example.

Traditional medicine practitioners widely use plant extracts as remedies for many ailments, including fever, inflammation, and infectious diseases. For instance, ayurvedic medicine provides countless examples of medicinally beneficial herbs containing phytochemicals, such as tannins, flavonoids, and alkaloids [1]. Previous reports have shown the benefits of the tannins and flavonoids against gram-positive cocci and *Candida albicans* infections [2, 3], and many alkaloids have been used clinically as anticancer agents, as highlighted by the use of vinca alkaloids for treating various lymphomas [1]. In the drug discovery process, screening for bioactive metabolites from known traditional herbs provides great medicinal interest, and different medicinal plant metabolites demonstrated a wide range of potential bioactivities, many of which found their way into clinical practice. A vast number of isolated plant metabolites in the form of crude mixtures exerted antimicrobial and cytotoxic potentials. However, due to the resistance of cancerous cells and microbes to the available medications, there is significant interest in identifying these metabolites [4, 5]. Among the plant secondary metabolites, alkaloids comprise a large group. Most of these agents contain heterocyclic nitrogen skeletons that, in some cases, such as with the pyridine alkaloids, resonate with an aromatic nucleus [6]. The importance of alkaloids in medicine is due to their potent pharmacologic effects at even low concentrations relative to other natural products. Their effects apply to various disorders, including bacterial and fungal infections and some cancers [7]. Pyridine alkaloids are essential members and have recorded medical benefits through demonstrating significant cytotoxic [8], antibacterial [9], and antifungal [10] effects. *Cyperus rotundus* L. (CR) is a herbaceous medicinal plant of the family Cyperaceae that grows in the Iraqi-Kurdistan Region of the Middle East. The CR crude extract (CE) has been used to treat many ailments, including fever, malaria, gastrointestinal disturbances, hormonal imbalances, and infections [11]. Sesquiterpenes [12], pyridine alkaloids [13], sterol glycosides [14], furochromones, and flavonoids [15] have been isolated from the CR rhizomes. Previous works investigating the cytotoxic [16], antibacterial [17], and antimycotic [18] activities of CR used the rhizomes' CEs rather than using single isolated compounds, as it is easier, more rapid, and less expensive. Despite the CR beneficial effects, the total extracts were used as remedies for the mentioned ailments; isolated purified entities as active constituents would potentially be more productive therapeutically due to their efficacy at very low concentrations and reduced intermolecular and intra-molecular interactions that may be associated with total extracts [19]. Rotundine alkaloids have been previously isolated from CR rhizomes, but no record of bioactivity has been reported [13]. The current study screened and evaluated a methanol extract of CR rhizomes to isolate and identify a potential bioactive pyridine alkaloid as a lead compound for anticancer and antimicrobials. The cytotoxic and antimicrobial effects of the alkaloid were then investigated.

Materials and Methods

Chemicals and reagents

High-performance liquid chromatography (HPLC) graded all chemicals and reagents to ensure precision and accuracy. Mueller Hinton Agar (MHA, LAB039) from Seoul, Korea, and Mueller Hinton Broth (MHB) from MD, USA, were prepared according to the supplier's recommendations. Sephadex LH-20 was purchased from GE Healthcare (USA), while gentamicin and fluconazole were obtained from TransGen Biotech (Beijing, China). Dulbecco's modified eagle's medium (DMEM), fetal bovine serum (FBS), trypsin, ampicillin, and kanamycin were purchased from TransGen Biotech (Beijing, China). Dimethyl sulfoxide (DMSO), 3-(4,5-dimethylthiazol-2-yl)-2,5-diphenyltetrazolium bromide (MTT), and 4′,6-diamidino-2-phenylindole (DAPI) were purchased from Karl Roth (Darmstadt, Germany). All the procedures were performed with consideration of laboratory safety operating procedures, chemicals, and biological samples were handled with extra care. The biological wastes were disinfected, autoclaved, and properly discarded. All chemicals were collected, detoxified, and properly discarded.

Bacterial and fungal strains and human cell line

Escherichia coli (ATCC No. 8739), *Staphylococcus aureus* (ATCC No. 6538), and *C. albicans* (ATCC No. 10231) were purchased from Medya-Med Labs (Erbil, Iraq). The bacterial strains were inoculated into fresh media, 10% glycerin was added, and aliquots were

stored at −80°C until use. The human endothelial HeLa cell line was obtained from the fine test (Wuhan, China). The HeLa cell line was thawed and inoculated into fresh DMEM containing 10% FBS in culture flasks and incubated at 37°C and 5% CO_2. Cell morphology and growth were checked every 24 h, and subsequently, sub-cultures were prepared.

Plant collection

CR plant was harvested from the Shahrazoor District, Sulaimaniyah-Iraq. Plant identification was carried out at the Kurdistan Botanical Foundation, and a voucher specimen was deposited in the Medicinal Plants Herbarium of the College of Pharmacy, University of Sulaimani, for future reference (voucher No.: Cr 17.01).

Extraction of plant material

The dried CR rhizomes were pulverized, and 250 g was treated with 10% alcoholic potassium hydroxide solution, which was then macerated in 350 mL methanol with shaking at 50°C for 72 h. The solvent was replaced with fresh solvent daily. The extract was filtered and vacuum-concentrated at 40°C in a rotary evaporator. The yield ([dried extract weight/crude plant weight]×100) was calculated, and the CE was re-suspended in 50 mL methanol. The solution was acidified using 1% hydrochloric acid, then vacuum filtered three times using the Whatman No.1 filter paper. The filtrate was extracted using methanol: chloroform (5:95 V:V). The pH adjustment to 9.0 was achieved by adding drops of ammonium hydroxide solution (35.046 g/mol).

Fractionation

The mixture was partitioned three times using 100 mL 5% methanol: chloroform. Sufficient volumes of Mayer's and Dragendorff's reagents were added to aliquots of the aqueous and organic layers on microscope slides, and the mixtures were observed under a microscope for the presence of precipitates. The organic phase was separated and vacuum condensed at 40°C. The final product was weighed and considered the crude alkaloid extract (CAE).

Column chromatography

The CAE was eluted over Sephadex LH-20 using 80 mL of methanol as an isocratic mobile phase. A total of 16×5 mL sub-fractions were collected. Each sub-fraction was tested for alkaloids using Mayer's and Dragendorff's reagents. Alkaloid-positive sub-fractions were subjected to thin-layer chromatography (TLC) analysis over silica gel using chloroform: methanol: Diethylamine at a volume ratio of 15:1:0.1. The chromatogram was sprayed with Dragendorff's reagents. Spots showing positive reactions (orange-brown color) were recovered using preparative-TLC, vacuum-dried, and again column-chromatographed under the same conditions as before, except smaller fraction volumes were collected (25×1 mL). A single spot that reacted positively with the alkaloid-detecting reagents was scraped and solubilized in 5 mL of 5% methanol: chloroform and then filtered. The solvent was evaporated at 40°C. An oily pale-yellow substance was recovered, weighted, and labeled as Alk-1. The Alk-1 sample was stored at 4°C until further analysis [13].

Total oligomer flavonoids analysis

An amount of one-hundred grams of the pulverized CR rhizomes were macerated using acetone: distilled water (2:1 V/V) at room temperature with shaking for 72 h. The solvent was refreshed daily. The extracts were pooled, filtered, and vacuum-condensed at 25°C. The aqueous phase was weighed and then treated with excess sodium chloride solution for 24 h at 5°C to remove the tannins. The obtained supernatant was extracted with ethyl acetate (EtOAc), and the extract was precipitated by adding an excess of chloroform. The precipitate was partitioned and dried, and the total oligomer flavonoids were calculated [20].

Determination of total flavonoid content

One-hundred grams of pulverized CR rhizomes were macerated in 70% ethanol at room temperature for 72 h. The CE was partitioned thrice with equal volumes of n-hexane, EtOAc, and n-butanol. One gram from the EtOAc portion was assayed for total flavonoid content using the aluminum chloride ($AlCl_3$) colorimetric method using quercetin as a standard. Aliquots from the CE and EtOAc fractions were prepared at 1 mg/mL concentrations. Serial dilutions of quercetin (10, 20, 40, 80, 120, and 160 µg/mL) were prepared in 95% ethanol as standard solutions adjusted with sterilized micropipettes. Then, 200 µL of each sample or standard was placed in a test tube and mixed with 0.1 mL of freshly prepared 10% $AlCl_3$, 0.1 mL $K^+(CH_3COO)^-$ solution, and 4.6 mL of distilled water. The mixture was vortex-mixed and left in the dark for 30 min. A blank was prepared for each sample using the same procedure, but distilled water was used instead of $AlCl_3$. The absorbance of the tubes at 415 nm was recorded using a UV-Vis spectrometer.

High-performance liquid chromatography analysis

The purity of the isolated alkaloid was determined using integrated HPLC analysis (Waters e 2695 Alliance HPLC systems, USA) with an Intersil C-18 column (150 mm×4.6 mm, 5 µm; GL Science, Japan). The chromatography was performed at 30°C using a mobile phase of acetonitrile: Distilled water at a 60:40 volume ratio and a 1 mL/min flow rate. The injection volume was 50 µL. The detection was performed at 254, 302, and 365 nm wavelengths. System precision, detector linearity, injector linearity and accuracy, injector carryover test, flow-rate linearity, compositional precision, noise, and drift test were previously tested for the instrument, and the method selection was based on previous literature [21]. The water used was purified using a Millipore Mill-Q system. The isolated alkaloid was stored at −86°C until structural elucidation and performance of bioactivity assays. Similar conditions and standard concentrations of authentic samples were applied in determining the amounts of nootkatone, quercetin, chlorogenic acid, catechin, and β-sitosterol in the CE.

Detection by chemical tests

One mg aliquot of the oily extract was tested with Mayer's and Dragendorff's reagents (dropwise addition), and the precipitate was examined under a microscope for confirmation.

Structure elucidation

Fourier-transform infrared (FTIR) spectrum analysis was performed using the KBr pellet method (Vmax in cm^{-1}) and a Perkin-Elmer FTIR spectrometer. Data interpretation was done using Spectrum-A software (ChemDraw Professional/ PerkinElmer, Ver. 19.1). The proton nuclear magnetic resonance (H-NMR) spectrum was recorded using an Avance-III 400 MHz NanoBay spectrophotometer (Bruker, Switzerland) and 2 mg of the alkaloid. The samples for chemical and biological analyses were dissolved in methanol. The following conditions were used: Spectrometer frequency=400.1500 MHz, acquisition time=4.0894465 s, relaxation delay (D1)=1.0 s, right pulse width=45°, spectral width=8012.820 Hz, digital resolution=0.3 Hz, and Fourier transform size=298.1 K. Chemical shifts (δ) were calculated as parts per million (ppm) relative to the D-glucose molecule ($CDCl_3$, δH 7.24, δC 77.0). The data were recorded using the Topspin software, version 3.2.

The mass spectrum analysis was applied using liquid chromatography with tandem mass spectrometry on an API-3200 system. The electrospray ionization technique was used, with the sample being directly injected with a continuous flow rate of 10 µL/mL for a total run time of 1 min. Ions were detected at a positive mode (m/z +1) using a carrying diluent of methanol: Distilled water (50:50 V/V), and the sample solution concentration was adjusted to 5 µg/mL. Detection parameters were DP=40, EP=10, IS=5500 v, and ion source spray gas 30. Data interpretation was done using the Analyst software, version 1.6.3.

Minimum inhibitory concentration and minimum bactericidal concentration assays

MIC values of the isolated compound were tested against non-fastidious microorganisms *S. aureus*, *E. coli*, and *C. albicans* according to the method previously established by the Clinical and Laboratory Standard Institute at a microbial cell density of 0.5×10^8 cells/mL. Briefly, the microorganisms were inoculated into sterile MHB and incubated for 24 h at 37°C. Microbial cultures were suspended in sterile normal saline (0.9%), and the concentrations were adjusted to an optical density of 0.5 McFarland turbidity standard [22]. Serial dilutions of the CE and the isolated compound were also prepared. The antibiotic gentamicin and antifungal fluconazole were used as standards, accordingly. The MIC assay was performed using sterile MHB with the microorganism cultures adjusted to 200 µL/well in 0.1% DMSO.

Preparation and dilution of stock solutions

Stock solutions were prepared in sterile test tubes with screw caps by dissolving 80 µg of each test sample or standard in 0.1% DMSO/sterile phosphate buffer saline to a final volume of 200 µL. The samples were then homogenized by vortex mixing. Each dilution was adjusted to a total volume of 200 µL/well, which included 50 µL serially diluted samples 1, 2, 4, 8, 16, 32, 64, and 100 µg/mL.

Bacterial sensitivity assay using microplate assembly

Sterile 96-well microplates were prepared with media alone (blank) or microbial suspension (20 µL/well, control) and serial dilutions of antibiotic or antifungal standards at concentrations of 1, 2, 4, 8, 16, 32, 64, and 100 µg/mL. Serial dilutions of aliquots of the isolated compound (1–100 µg/mL) were added to the blank and microbial suspensions. Each well was adjusted to a total volume of 200 µL using micropipettes. The plates were incubated overnight at 37°C with shaking adjusted to 200

rounds per minute. The plates were then examined for bacterial growth, and readings were taken at 600 nm using an enzyme-linked immunosorbent assay microplate reader. The tests were performed in triplicate [23]. To determine the MBCs, inoculated samples from dilutions showing bacterial inhibition onto MHA plates were incubated overnight at 37˚C and then examined for bacterial growth [23]. The blank, which included the growth medium, was used only as background, and the control included the growth medium with cultures of the tested microorganisms.

Determination of cytotoxicity using MTT cell proliferation assays

The isolated compound's cytotoxicity and cell viability were determined using MTT cell proliferation assays. HeLa cells were seeded into culture flasks containing DMEM supplemented with 10% FBS, ampicillin (1 µL/mL), and kanamycin (0.5 µL/mL) and incubated in a humidified atmosphere of 5% CO_2 at 37˚C. Sub-cultures were prepared on alternate days when confluence reached 70%, and cell morphology was examined. The HeLa cells were inoculated into sterile 96-well microplates at a density of 1×10^4 cells/well and incubated at 37˚C for 24 h in a 5% CO_2 incubator. Following incubation, the cells were examined for adherence and morphology and then treated with serial dilutions of the isolated compound at concentrations of 20, 40, 80, 160, and 200 µg/mL. The blank consisted of DMEM supplemented with 10% FBS (cell-free), while the control was media + HeLa cells [16]. The absorbance values of the blank wells were subtracted as background from the absorbance values of the sample wells, and the IC_{50} values were calculated. The plates were incubated for 24 h under the same conditions. The culture media and the treatment dilutions were then replaced with freshly prepared BSA-free DMEM MTT reagent added to each well (0.5 mg/mL) and incubated for 4 h at 37˚C. DMSO (100 µL) was then added to dissolve the developed formazan crystals, and the absorbance of each well was measured at 540 nm using an enzyme-linked immunosorbent assay microplate reader. The absorbance values of the blank wells were subtracted as background from those of the sample wells, and the IC_{50} was calculated. Each assay was performed in triplicate.

DAPI assay

DAPI dye was prepared by dissolving 20 mg of the pigment in 1 mL of distilled water. The suspension was homogenized in the dark with sonication using an ultrasonic water bath. The solution was stored at 4˚C until use. HeLa cells were incubated in a humidified ambient environment with 5% CO_2 at 37˚C for 24 h. After adherence, the cells were treated with the isolated compounds at 20–200 µg/mL concentrations and then fixed for 15 min in 4% paraformaldehyde, followed by washing with PBS. The DAPI dye was added to the cells (control and treated) and left undisturbed in the dark for 5 min. Chromatin changes (apoptosis) were then recorded using an inverted fluorescence microscope [24].

Statistical analyses

All experiments were independently performed four times, and the data were expressed as Mean±SD. Statistical analysis was carried out using one-way analysis of variance followed by the Tukey post hoc test of the MTT assay results with nonlinear regression analysis of the IC_{50} results. Differences were considered statistically significant at $P<0.05$.

Results

Phytochemical characterization of the crude extract

The CAE yield comprised 0.016% of the total CE, while the isolated oily Alk-1 obtained by column chromatography (R_F=0.4) was 20 mg, which was 0.008% of the total weight of the rhizomes CE (Table 1). Total oligomer flavonoids and total flavonoid content results and the amounts of nootkatone, quercetin, chlorogenic acid, catechin, and β-sitosterol according to HPLC analysis are shown in Table 1. HPLC analysis of the isolated compound showed a retention time (R_T) of 3.0 with a single peak (Figure 1a).

Table 1. Physicochemical characterization of the crude extract of CR rhizomes and the crude extract fractions

Percentage of Crude Alkaloid Extract in the Methanolic CE of CR Rhizomes					
CRW (g)	Yield (g)	Alkaloid Extract (g)	CAE%	Alk-1 (g)	% Alk-1
250	16	0.04	0.016	0.02	0.008

TOF Percentage Obtained From the CE of CR Rhizomes	
Weight (g)	**Yield (%, w/w)**
CE	8.9
TOF	0.12

TFC of the CE of CR Rhizomes and Its Partitions (µg) out of (mg) Fraction Weight				
Mean±SE				
CE	**Hexane**	**Ethyl acetate**	**Butanol**	**Aqueous**
110.57±0.9	21.88±0.8	54.91±0.1	6.33±0.5	13.85±0.4

HPLC Analysis of the Chemical Constituents of CE and EtOAc Methanolic Extracts of CR Rhizomes (µg/mL) Compared to Standards						
Chemical Constituents	**RT**	**Weight**		**SE**	**Weight**	**SE**
	min	**Std.**	**Crude Extract**		**Ethyl Acetate**	
Nootkatone	7.988	0.5	0.1165	0.0003	0.0150	0.0067
Quercetin	1.728	0.5	0.8432	0.0677	0.0010	0.0003
Chlorogenic acid	1.315	0.5	0.6368	0.0297	-	-
Catechin	1.249	1.0	0.0765	0.0003	0.145	0.0020
β-Sitosterol	9.308	1.0	0.2540	0.0012	-	-

Abbreviations: CAE: Crude alkaloid extract; CRW: Crude rhizomes weight; Alk-1: Isolated alkaloid compound 1; CE: Crude extract; SE: Standard error; RT: Retention time; Std: Standard sample; TOF: Total oligomer flavonoids; TFC: Total flavonoid content; EtOAc: Ethyl acetate; CR: *Cyperus rotundus*.

Table 2. Fourier-transform infrared spectra absorption bands, %T vs cm^{-1} for the isolated compound (Alk-1)

Absorbance (cm^{-1})	Possible Functional Group
3550	C-H stretching of free hydroxyl groups (sugar)
3064, 3032	C-H stretching of aromatic compounds
2929	C-H stretching of the alkyl group
2873	C-H stretching of aliphatic ($-CH_2$, $-CH_3$)
2000–1700	Overtone aromatic
1602	C-C stretching of aromatic activated ring (possibly pyridine)
1498	C-C bending of aromatic
1390	C-H bending (Sp^3)
1255	C-O stretching of ether, alcohol
1100–1000	C-O alkoxy
800	C-H bending (Sp^2)
728, 693	Bending (out of plane) of aromatic compounds
462	Traces of halogen (chloroform)

Abbreviations: C-H: Carbon-hydrogen bond; C-C: Carbon-carbon bond; Sp^3: Orbital hybridization; C-O: Carbon-oxygen bond.

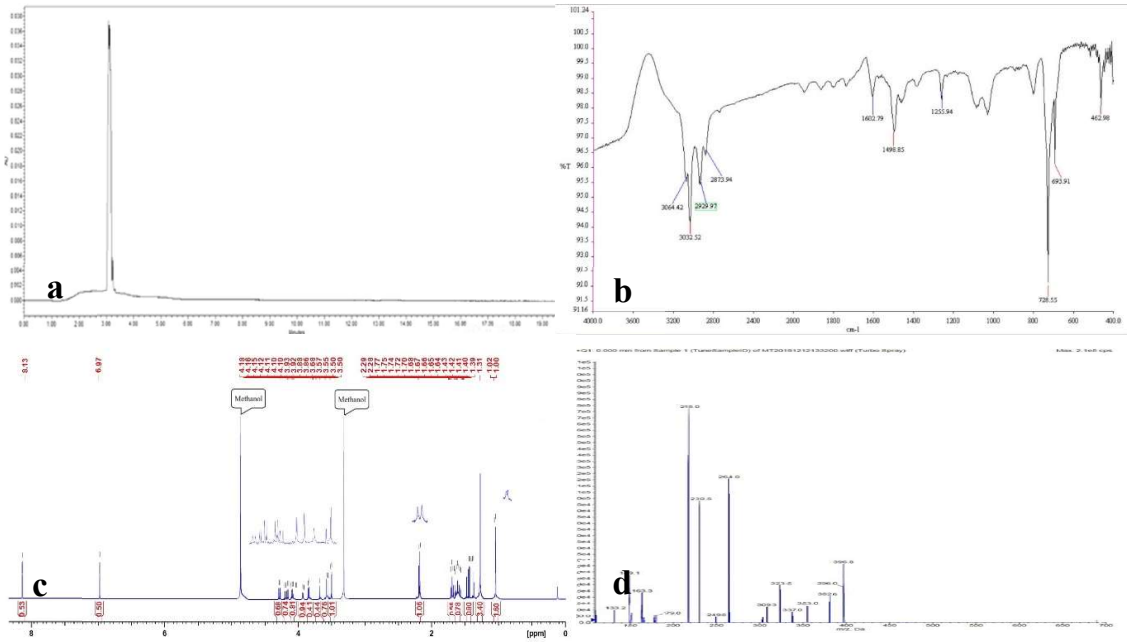

PBR

Figure 1. Physicochemical characterization of the compound Alk-1 isolated from the crude extract of CR rhizomes

Notes: a) High-performance liquid chromatography chromatogram of the isolated compound Alk-1 ran through C-18 reversed-phase column using acetonitrile: Water 60:40 V: V, showing a single peak at Rt of 2.0; b) Fourier-transform infrared spectrum using KBR pellets, the spectrum was recorded as absorbance vs cm^{-1} for the isolated alkaloidnorrotundine-6-O-glucoside; c) The chemical shift (ppm) of the isolated alkaloidAlk-1 based on proton nuclear magnetic resonance spectrum chart (400 MHz, methanol); d) Mass spectrum analysis ofnorrotundin-6-O-glucoside.

The reproduction size for each figure is 1/8.

Fourier-transform infrared analysis

FTIR assay results are illustrated in Figure 1b and Table 2. FTIR spectrum revealed a broadband at 3550 cm^{-1}, which indicates an absorbance due to O-H stretching of multiple alcoholic hydroxyl groups, primarily glucose hydrogens bonded with water. Furthermore, the strong broadband suggested intermolecular bonding. The absorption at 1375 cm^{-1} is for O-H stretching of the multiple glucose hydroxyls. A band at 1255 cm^{-1} for C-O stretching of ether supported the presence of alcohol, most likely for the sugar-free hydroxyl alcohol groups [25]. The peak at 2873 cm^{-1} is for C-H stretching of aliphatic hydrocarbons (-CH_2, -CH_3). The bands at 3064 cm^{-1}, 3032 cm^{-1}, and 2929 cm^{-1} were the results of C-C stretching of aromatic compounds, further supported by an overtone at 2000–1700 cm^{-1} and a C-C stretching at 1602 cm^{-1}. The shift in absorbance can be attributed to ring activation by the nitrogen atom, which is typical for pyridine. This was evidence for the presence of pyridine rather than benzene. The band at 1498.85 cm^{-1} demonstrates the C-C bending of aromatic compounds, while the absorbance at 728 cm^{-1} and 693 cm^{-1} (out-of-plane bending) were due to multiple aromatic substitutions. The band at 462 cm^{-1} was the result of traces of halogens from the solvent (chloroform). The free alcoholic hydroxyl proton of the Alk-1 at C-14 was overlapped by the glucose hydroxyls [26, 27].

Proton nuclear magnetic resonance analysis

Assignment of the protons was done using H-NMR (400 MHz, methanol, d) with the integration calculated for each proton as (H^+=0.5), according to the glucose protons. The results for Alk-1 showed the following δs: 1.00 (d, J=4 Hz, 3 H), 1.31 (s, 6 H), 1.4 (m, J=4 Hz, 2 H), 1.64 (m, J=8.0 Hz, 2 H), 1.7 (m, J=164 Hz, 1 H), 2.28 (d, J=4.0 Hz, 2 H), 3.5 (d, 2 H), 3.55 (d, 2 H), 3.68 (s, 1 H), 3.86 (d, 1 H), 3.92 (d, 1 H), 4.1 (m, 2H), 4.15 (d, 1 H), 4.16 (d, 1 H), 3.5-4.16 (m, J=8 Hz, 11 H), 6.97 (d, 1 H), 8.13 (d, 1 H) (Figure 1c). The δ at 8.13 ppm, s (1 H) and δ at 6.97 ppm, *s* (1 H) were caused by the protons attached to C-2 and C-5 of the pyridine ring, respectively. The proton appeared downfield (>8.0 ppm) as the ring was activated. The proton attached to C-2 appeared in the lower field as it was also adjacent to the nitrogen atom [25, 27]. The pyridine ring was substituted with a cyclopentane ring at C-3 and C-4. The two C-7 pro-

Table 3. Absorbance (nm) of *S. aureus* cultures as an indicator of the antimicrobial effect of the isolated compound (Alk-1) at various concentrations relative to gentamicin and the control and blank

Experiments		Absorbance (nm) Concentration (µg/mL) 1	2	4	8	16	32	64	100	Microorganisms
Alk-1	EXP 1	1.020	0.760	0.645	0.561	0.421	0.238	0.076	0.077	*S. aureus*
	EXP 2	0.990	0.778	0.630	0.545	0.437	0.213	0.069	0.067	
	EXP 3	0.970	0.798	0.680	0.570	0.449	0.241	0.072	0.063	
	∑	2.980	2.336	1.955	1.676	1.307	0.692	0.217	0.207	
	Mean	0.993	0.779	0.652	0.559	0.436	0.231	0.072	0.069	
	SE	0.335								
Gentamicin		0.098	0.072	0.069	0.064	0.059	0.058	0.056	0.050	
Blank		0.059	0.060	0.058	0.051	0.057	0.051	0.063	0.054	
Control		0.810	0.790	0.800	0.830	0.770	0.850	0.690	0.790	
Alk-1	EXP 1	0.700	0.580	0.410	0.320	0.340	0.219	0.187	0.102	*E. coli*
	EXP 2	0.659	0.620	0.460	0.370	0.270	0.247	0.157	0.089	
	EXP 3	0.680	0.570	0.450	0.390	0.290	0.249	0.164	0.081	
	∑	2.039	1.770	1.320	1.080	0.900	0.715	0.508	0.272	
	Mean	0.680	0.590	0.440	0.360	0.300	0.238	0.169	0.091	
	SE	0.203								
Gentamicin		0.068	0.056	0.053	0.048	0.043	0.040	0.040	0.039	
Blank		0.059	0.060	0.052	0.065	0.049	0.059	0.057	0.056	
Control		0.268	0.328	0.580	0.332	0.364	0.694	0.916	0.504	
Alk-1	EXP 1	0.972	0.932	0.802	0.701	0.518	0.323	0.147	0.071	*C. albicans*
	EXP 2	1.064	0.946	0.794	0.696	0.496	0.354	0.140	0.069	
	EXP 3	1.190	0.904	0.870	0.709	0.549	0.341	0.125	0.060	
	∑	3.226	2.782	2.466	2.106	1.563	1.018	0.412	0.200	
	Mean	1.075	0.927	0.822	0.702	0.521	0.339	0.137	0.067	
	SE	0.370								
Fluconazole		0.089	0.081	0.076	0.060	0.057	0.051	0.048	0.039	
Blank		0.051	0.089	0.765	0.056	0.052	0.053	0.051	0.090	
Control		0.927	0.908	1.040	0.947	0.987	0.912	0.879	1.040	

PBR

Abbreviations: Alk-1: Isolated alkaloid compound; EXP: Experiment; SE: Standard error; Blank: Growth media alone; Control: Growth media and bacterial strain growth cultures.

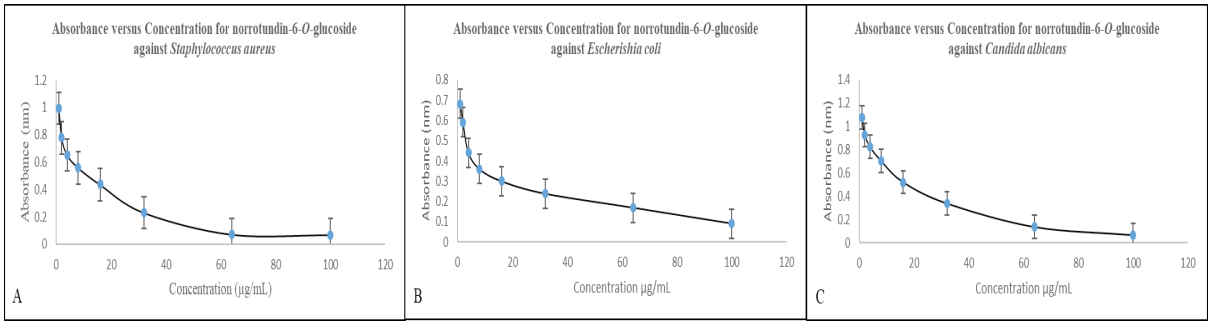

Figure 2. The inhibitory effect of the isolated alkaloid (Norrotundin-6-O-glucoside) on growth of (a) *S. aureus*, (b) *C. albicans*, and (c) *E. coli* at concentrations of 1–120 µg/mL

Notes: The reproduction size of each figure is 1/15.

tons appeared in the region 2.28 ppm, d (2 H) and were coupled (J=4.0 Hz). These two protons split the C-8 proton (J=164 Hz), shown in the region 1.77 ppm, m. The protons of the two methyl groups (C-10 and C-11) attached to C-9 of the cyclopentane appeared in the region 1.31 ppm, s (6 H). These were adjacent and symmetric, displaying the same integration (geminal protons). The assigned 2-butanol protons attached to the cyclopentane ring at C-8 showed δ at 1.64 ppm, m (2H) for the C-13 protons. These protons appeared in this region as they were adjacent to the alcoholic C-14, adjacent to each other and coupled (J=8.0 Hz), and split the protons attached to C-12 and C-14 (J=88.0 Hz). The broad multiplet peak below 2.0 ppm was from the C-14 proton being un-shielded by the alcoholic hydroxyl. The alcoholic hydroxyl proton attached to C-14 overlapped with the alcoholic or glucose hydroxyl protons as they appeared in the same region [25]. The C-12 protons appeared in the region 1.42 ppm, m (2 H). These protons were coupled and adjacent to each other (J=4 Hz). The three protons attached to C-15 appeared in the upfield region at 1.0 ppm, d (3 H), and were coupled to each other (J=4 Hz).

The H-NMR analysis showed the presence of glucose protons in the region 4.3–3.5 ppm (11 H). The proton attached to the sugar anomeric carbon sugar was shielded and appeared downfield for the adjacent electronegative oxygens (anomeric and C-5′). The C-(2′, 5′) protons were shifted downfield because of the neighboring oxygen atoms. These protons overlapped with the methanol (solvent) proton and appeared in the region 4.16-3.5 ppm. The two protons attached to C-6′ appeared in the region 3.49-3.51 ppm, d (1 H) and split each other and the adjacent hydroxyl proton (H-C-OH; J=8.0 Hz).

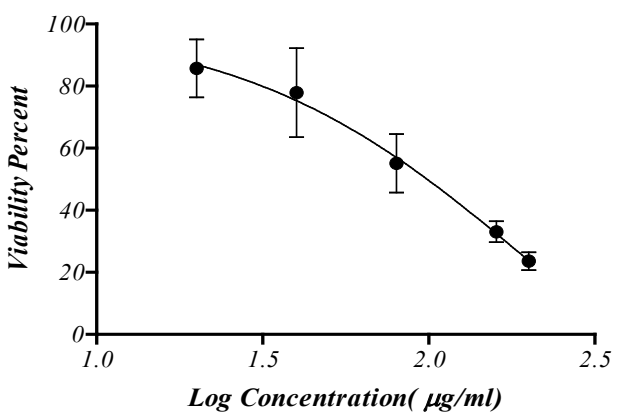

Figure 3. The MTT assay chart showing the percentage of viable HeLa cells, a human epithelial cell line, upon in vitro assessment of the cytotoxicity of the isolated Norrotundine-6-O-glucoside compound (indicated in log concentration [µg/Ml])

Notes: The vertical lines represent standard error. The IC_{50}=203.7 µg/mL.

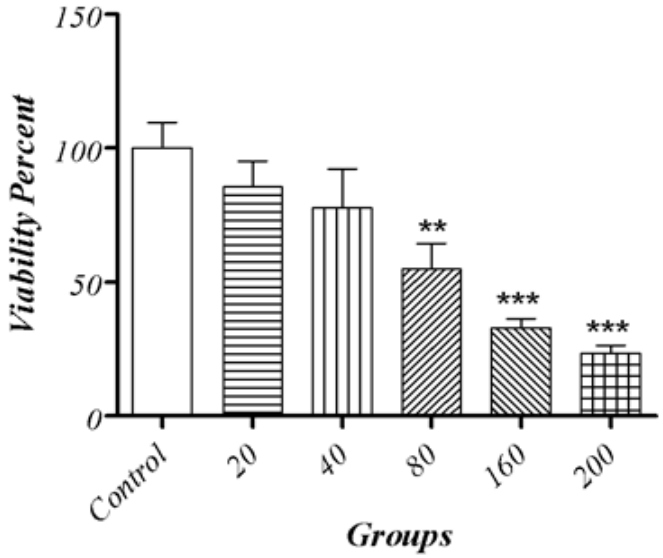

PBR

Figure 4. Percentage of viable HeLa cells treated with the isolated Norrotundine-6-O-glucoside compound at various concentrations (20–200 µg/mL); IC_{50}=203.7

Notes: The data are shown as an mean of six repeats (in each group) ±standard error; **P<0.01 and ***P<0.001.

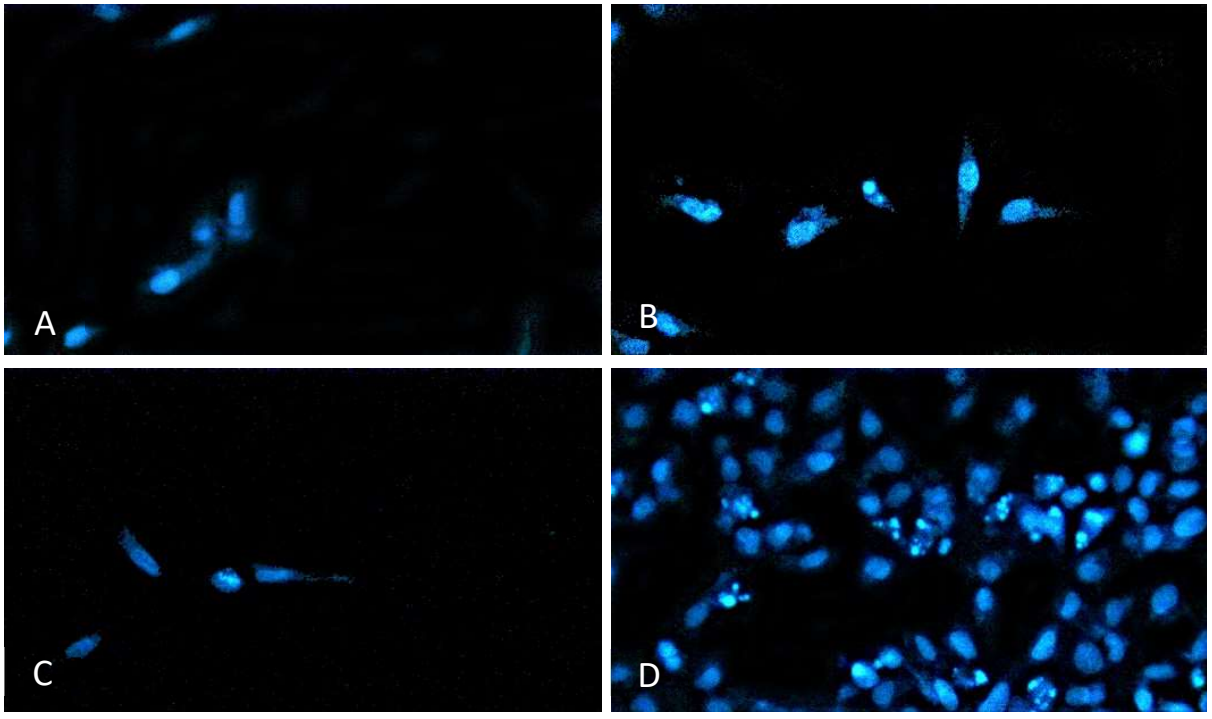

PBR

Figure 5. Morphology and density of in vitro culture of HeLa cells stained with DAPI observed under cell imager with 20× objective lens of phase contrast inverted fluorescent microscope after 24 h

a-c) Cells treated with increasing concentrations of the isolated norrotundine-6-O-glucoside (1–200 µg/mL); d) Control (untreated cells)

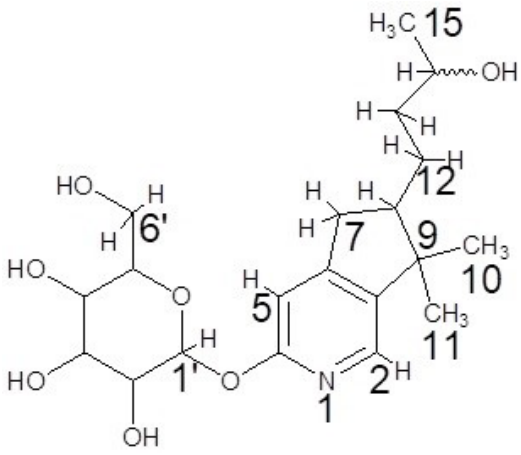

PBR

Figure 6. Chemical formula of the compound Norrotundine-6-O-glucoside (Alk-1) isolated from the methanolic crude extract of CR
Notes: The chemical formula was drawn using the Chem Office.

Mass spectrum analysis

The mass of the molecular ion for the isolated Alk-1 was M^+=397. The other ion fragments are shown in Figure 1d. Mass spectrum analysis of the isolated Ak-1 ($C_{20}H_{31}NO_7$) using the high-resolution LC-MS/MS ABSCIEX system revealed ion fragments m/z 163 and m/z179 for glucose-OH. The mass spectrum analysis also showed the fragment mz=396.6 (M^+).

Antimicrobial assays (minimum inhibitory concentrations (MIC) and minimum bactericidal concentrations assays (MBC))

MIC analysis of the Alk-1 compound against *S. aureus* showed that it inhibited bacterial growth at a 64 µg/mL concentration. The results for the MBC assay mean was 64 µg/mL with no growth being detected (bactericidal). The same results were seen at higher concentrations of the Alk-1. The MIC for Alk-1 against *E. coli* was 100 µg/mL. No inhibition of *E. coli* was detected in the MBC assay at the same concentration. The antifungal activity of Alk-1 against *C. albicans* was recorded as 64 µg/mL, and no growth (fungicidal) was detected in the MBC assay (Figure 2 and Table 3). The MIC assays for Alk-1 against both *S. aureus* and *C. albicans* showed increased inhibition with increasing concentrations from 64 µg/mL to 100 µg/mL. The same results were obtained for the MBC assays against the tested microorganisms, with no growth detected on the agar plates; however, the antibacterial activity of Alk-1 against *E. coli* was seen only at 100 µg/mL, with no apparent inhibition of growth on the agar plates. The blank wells showed no growth, and the control wells showed no inhibition. The MIC and MBC assay results of the tested alkaloid showed selective bactericidal activity against *S. aureus* and *C. albicans*, while bacteriostatic action against was observed against *E. coli*.

Cytotoxicity assays

MTT assays

The MTT assay results showed significant activity at 80 µg/mL and highly significant cytotoxicity at 160–200 µg/mL for the isolated Alk-1 against HeLa cells. The IC_{50} value was 203.7 for Alk-1 (Figure 3). As shown in Figure 4, the results of the cell viability analysis in response to increasing concentrations of the test compound showed a significant decrease (P=0.0133) in the cell numbers. For both antimicrobial and cytotoxicity assays, low concentrations were considered to show clinical significance and productivity compared to human utilization and eligible pharmaceutical dosage formulations.

DAPI analysis

The DAPI assay results showed morphological changes, including chromatin changes in treated cells with the isolated compound, condensed chromatin, fragmented nuclei, and apoptotic bodies. These effects are characteristics of apoptosis and were dose-dependent, as shown in Figure 5.

Discussion

The relative amount of CAE (0.016%) obtained from the CE of CR rhizomes followed the results obtained previously (0.017%) [13]; however, the percentage of the isolated alkaloid per extract weight in our study (0.008%) was 2.5-fold higher compared to that of previous reports [13]. This difference may be accredited to a longer extraction period and an elevated extraction temperature with shaking. The amounts of nootkatone were 20-fold less in the current study compared to previous studies [18], which may be attributed to differences in the detection method, plant echo system, extraction, and isolation processes. The amounts of quercetin, chlorogenic acid, catechin, and β-sitosterol in the CEs and EtOAc fraction also showed variations compared to the previous reports. Earlier studies detected these compounds in the CE. Still, the results of the current study differed in the type and quantity of each component, likely due to environmental factors, the solvents used, and the techniques applied in the extraction and isolation processes [20, 28-30]. In this work, the polyphenolic contents (TOF and TFC) were obtained from the EtOAc fraction, while previous studies assayed the total extract [20, 31-33]. This might have caused the three-fold decrease in yields in the amounts of polyphenols in the current study compared to the previous reports.

The δ pattern from H-NMR analysis previously presented for rotundine B [13], an alkaloid isolated from CR rhizomes (not glycosylated), is highly relevant to our current results. Variations in the proton shifts may be attributed to the isolated compound due to the glycosylation effect on the solubility and the overlapping of alcoholic hydroxyl protons with the alcoholic hydroxyl at C-14. Furthermore, glycosylation may affect the structural pattern of the attachment of pyridine and the cyclopentane ring at C-3 and C-4, which varied in our study compared to that reported in the previous study [13]. Structural elucidation of the isolated compound illustrated the chemical formula of the oily yellow alkaloid, which was also confirmed by the positive reaction to alkaloid-detecting reagents.

The structural variation of Alk-1 (norrotundin-6-O-glucoside) compared with the previously reported rotundine B [34] may be attributed to differences in the growth conditions and environmental changes that may affect protein expression and modify biogenetic assemblies. This may contribute to further post-translation modification involving the addition of a glucose moiety by glucosyltransferase (Figure 6). The final metabolite should serve a biological purpose to the plant [35].

S. aureus, *E. coli*, and *C. albicans* are opportunistic pathogens and are the common causes of a wide range of infections in the community in general and hospitalized patients particularly. The increased resistance to antimicrobial agents is a trait related to biofilm formation, and these organisms are all capable of producing biofilm, especially on prosthetic materials and catheters, contributing to great risk in immunocompromised patients.

The antimicrobial activity of the isolated compound Alk-1 showed inhibitory activity against *S. aureus* at 64 μg/mL with no growth on MHA plates at this concentration, indicating it was bactericidal [17]. The detected MIC against *E. coli* was 100 μg/mL, and the MBC assay exhibited bacteriostatic activity. The MIC and MBC values were 64 μg/mL against *C. albicans*. Previous studies demonstrated antimicrobial activity for the CE from CR rhizomes [17]. However, there are no reports about testing the antimicrobial properties of isolated rotundine. Previous studies have shown relevant antibacterial activities of different carbazole alkaloids against *S. aureus* with an isolated harman dianamine having an MIC value of 64 μg/mL. At the same time, other related isomers express greater antibacterial potency [36]. The noticeable antimicrobial effects of Alk-1 against *S. aureus* and *C. albicans* suggest that this compound should be tested against multi-drug-resistant species of the same microorganisms. As the initial study using whole plant extract demonstrated activity only against the gram-positive bacteria *S. aureus* and the yeast *C. albicans*, the purified compound was also expected to exhibit activity against only these two microorganisms. The absence of an inhibitory effect of the CE against *E. coli* growth may be attributed to inter, or intra-molecular deactivation of the mixture components, leading to lower activity than the purified compound.

Earlier studies investigated the CR rhizomes' CE cytotoxicity and recorded activity against various human cancer cell lines, but they failed to attribute the activity to any specific metabolite [16, 37]. Screening for molecules showing cytotoxic properties is inevitable because of the high global mortality rates caused by different cancer types [34]. In the current study, evaluation of the isolated norrotundine-6-O-glucoside demonstrated dose-dependent cytotoxicity against HeLa cells, a human endothelial cancer cell line at 80 μg/mL, with increased activity at 160–200 μg/mL and an IC_{50} of 203.7 μg/mL after exposure to increasing concentrations (20–200 μg/mL). Evidence of condensed chromatin, fragmented nuclei, and formation of apoptotic bodies were all observed, in which chromatin condensation can be regarded as the normal transformation stages of genetically

active chromatin to an inactive highly condensed form, followed by fragmentation and packaging into apoptotic bodied during apoptotic execution [38]. The mechanisms underlying the desensitization of mutated cells to apoptotic proteins may be attributed to intrinsic and extrinsic factors. Studies on cancer molecular targeting are focused on resetting apoptotic sensitization through the studying various proteins involved in this cascade, such as the anti-apoptotic Bcl-2, FLICE-inhibitory protein, c-FLIP, inhibitor of apoptosis proteins, and caspases [39]. The cytotoxic effect of CR rhizome extract has been evaluated previously, and the results showed promising cytotoxicity against various cancer cell lines [16]. HeLa cells have been used to develop many drugs and treatments and have been instrumental in gene mapping and studying human diseases, especially cancer. Our current study showed concentration-dependent cytotoxicity and enhanced apoptosis by the isolated alkaloidal glycoside. However, previous studies have reported lower IC_{50} values for different isolated alkaloids against HeLa cells. For instance, the steroidal alkaloids tomatidine and solasodine inhibit HeLa cells with IC_{50} values at 146.5 µg/mL and 104.3 µg/mL, respectively [22]. In contrast, other alkyl pyridine alkaloids inhibit HeLa cells at even lower concentrations (IC_{50}=9.07 µg/mL) [40]. This study's lower cytotoxic potency of the isolated norrotundine-6-O-glucoside may be attributed to lower penetration capacity than the previously reported alkaloids. Such variations in the alkaloid's cytotoxicity could be greatly influenced by their diverse chemical structures and cellular macromolecular targeting sites. The observed differences in the current study compared to previous ones in terms of the amount and types of the screened metabolites providing that various environmental conditions and separation techniques are applied, such findings emphasize the capacity of living systems like plants to adapt to unusual conditions through new proteins transcriptions with modified functions to evolve new compounds with new therapeutic potentials.

Conclusion

This study was limited by insufficient data analysis of the isolated alkaloid, which was not previously characterized for chemical structure and biological activities. There is need to extend the antimicrobial activity to include a broad spectrum of resistant strains (Ex: Vancomycin-resistant *enterococcus*, *Acinetobacter baumannii*, *Pseudomonas aeruginosa*, and *Campylobacter* spp.) and examine the IC_{50} of the isolated compound against more human cancer cell lines (Ex: breast [MCF-7], colorectal [HT-29], liver [Hep G2], and prostate [PC-3]). There is also a need for further structure elucidation of the isolated compound to identify its stereoisomers.

The plant used in our current study, *C. rotundus*, is a naturally growing weed in the Kurdistan Region of Iraq. The use of sequential extraction and chromatographic techniques, and spectroscopic analysis using FTIR, H-NMR, and MS led to the isolation of a novel rotundine glycoside from the methanolic crude extract of the plant rhizomes; such finding demonstrated for the first time the presence of a glycoside and positioning of the attachment to the alkaloid nucleus as a structural variation from the previously reported compound. The antimicrobial and cytotoxic assessments were not tested previously for the isolated alkaloid. Furthermore, previous studies examined galenic crude extract rather than a purified compound's activity assessment, which is more beneficial for the drug discovery process. The isolated rotundine glycoside norrotundine-6-O-glucosidemaybe an excellent candidate antimicrobial and or anticancer drug. However, extended studies are required to confirm its potential. This compound may also be useful as a biomarker for the chemotaxonomic identification of the plant based on the isolated metabolite expressed by this plant species.

The need for new cytotoxic compounds should further drive investigations in the drug discovery field to unravel the relationship between structure and activity of norrotundine-6-O-glucoside. Furthermore, greater insight is needed regarding the molecular mechanism behind the cytotoxicity of norrotundine-6-O-glucoside, such as transcriptional analysis of the genes involved in its induction of the apoptotic pathway and molecular targeting sites involved in the cell toxicity, which includes the proteins involved in cell proliferation, enzymes modulating the DNA or extranuclear factors.

Ethical Considerations

Compliance with ethical guidelines

There were no ethical considerations to be considered in this research.

Funding

This research was supported by the University of Sulaimani (Grant No.: 7/2/13319).

Authors' contributions

Conceptualization and Supervision: Kawkab Y. Saour and Shwan Rachid; Methodology: Mohammed N. Sabir; Investigation, Writing – original draft, and Writing – review & editing: Mohammed N. Sabir; Selar Izzat; Bahez O. Ismael; Shwan Rachid; Data collection: Shahlaa M Abdullah; and Bahez O. Ismael; Data analysis: Mohammed N. Sabir; Selar Izzat and Shahlaa M Abdullah.

Conflict of interest

The authors declared no conflict of interest.

Acknowledgments

The authors express their appreciation to the University of Sulaimani for supporting this research. The authors would also like to extend their gratitude to both Emad M. Al-Khafaji and Sewara Jalal for their cooperation and to all who contributed to this work. Profound appreciation to Pioneer Company for Pharmaceutical Industries-Sulaymaniyah/Iraq for help performing the high-performance liquid chromatography analysis.

References

[1] Singh DB, Pathak RK, Rai D. From traditional herbal medicine to rational drug discovery: Strategies, challenges, and future perspectives. Rev Bras de Farmacogn. 2022; 32(2):147-59. [Link]

[2] Bylka W, Matlawska I, Pilewski N. Natural flavonoids as antimicrobial agents. JANA. 2004; 7(2):24-31. [Link]

[3] Buzzini P, Arapitsas P, Goretti M, Branda E, Turchetti B, Pinelli P, et al. Antimicrobial and antiviral activity of hydrolysable tannins. Mini Rev Med Chem. 2008; 8(12):1179-87. [DOI:10.2174/138955708786140990] [PMID]

[4] Saleem M, Nazir M, Ali MS, Hussain H, Lee YS, Riaz N, et al. Antimicrobial natural products: An update on future antibiotic drug candidates. Nat Prod Rep. 2010; 27(2):238-54. [DOI:10.1039/B916096E] [PMID]

[5] Nussbaumer S, Bonnabry P, Veuthey JL, Fleury-Souverain S. Analysis of anticancer drugs: A review. Talanta. 2011; 85(5):2265-89. [DOI:10.1016/j.talanta.2011.08.034] [PMID]

[6] Bribi N. Pharmacological activity of Alkaloids: A review. Asian J Bot. 2018; 2(1):1-6. [Link]

[7] Kaur R, Arora S. Alkaloids-important therapeutic secondary metabolites of plant origin. J Crit Rev. 2015; 2:1-8. [Link]

[8] Hirano K, Kubota T, Tsuda M, Mikami Y, Kobayashi J. Pyrinodemins B-D, potent cytotoxic bis-pyridine alkaloids from marine sponge amphimedon sp. Chem Pharm Bull. 2000; 48(7):974-7. [DOI:10.1248/cpb.48.974] [PMID]

[9] Chelossi E, Mancini I, Sepcić K, Turk T, Faimali M. Comparative antibacterial activity of polymeric 3-alkylpyridinium salts isolated from the mediterranean sponge reniera sarai and their synthetic analogues. Biomol Eng. 2006; 23(6):317-23. [DOI:10.1016/j.bioeng.2006.09.005] [PMID]

[10] Rinez A, Daami-Remadi M, Omezzine F, ladhari A, Rinez I, Haouala R. Assessment of the antifungal activity of nicotiana glauca Graham aqueous and organic extracts against some pathogenic and antagonistic fungi. Afr J Microbiol Res. 2012; 6(22):4655-61. [DOI:10.5897/AJMR11.979]

[11] Al-Snafi AE. A review on Cyperus rotundus a potential medicinal plant. IOSR J Pharm. 2016; 6(7):32-48. [DOI:10.9790/3013-06723248]

[12] Hu QP, Cao XM, Hao DL, Zhang LL. Chemical composition, antioxidant, DNA damage protective, cytotoxic and antibacterial activities of Cyperus rotundus rhizomes essential oil against foodborne pathogens. Sci Rep. 2017; 7:45231. [DOI:10.1038/srep45231] [PMID] [PMCID]

[13] Jeong SJ, Miyamoto T, Inagaki M, Kim YC, Higuchi R. Rotundines A-C, three novel sesquiterpene alkaloids from Cyperus rotundus. J Nat Prod. 2000; 63(5):673-5. [DOI:10.1021/np990588r] [PMID]

[14] Sayed HM, Mohamed MH, Farag SF, Mohamed GA, Proksch P. A new steroid glycoside and furochromones from Cyperus rotundus L. Nat Prod Res. 2007; 21(4):343-50. [DOI:10.1080/14786410701193056] [PMID]

[15] Kumar KH, Razack S, Nallamuthu I, Khanum F. Phytochemical analysis and biological properties of Cyperus rotundus L. Ind Crops Prod. 2014; 52: 815-26. [DOI:10.1016/j.indcrop.2013.11.040]

[16] Mannarreddy P, Denis M, Munireddy D, Pandurangan R, Thangavelu KP, Venkatesan K. Cytotoxic effect of Cyperus rotundus rhizome extract on human cancer cell lines. Biomed Pharmacother. 2017; 95:1375-87. [DOI:10.1016/j.biopha.2017.09.051] [PMID]

[17] Parekh J, Chanda S. In-vitro antimicrobial activities of extracts of Launaea procumbens roxb. (Labiateae), Vitis vinifera l. (Vitaceae) and Cyperus rotundus l. (Cyperaceae. Afr J Biomed Res. 2006; 9(2):89-93. [DOI:10.4314/ajbr.v9i2.48780]

[18] Sharma SK, Singh AP. Antimicrobial investigations on rhizomes of Cyperus rotundus linn. Der Pharm Lettre. 2011; 3(3):427-31. [Link]

[19] Johnson-Ajinwo OR, Richardson A, Li WW. Cytotoxic effects of stem bark extracts and pure compounds from Margaritaria discoidea on human ovarian cancer cell lines. Phytomedicine. 2015; 22(1):1-4. [DOI:10.1016/j.phymed.2014.09.008] [PMID]

[20] Kilani S, Bouhlel I, Ben Ammar R, Ben Shair M, Skandrani I, Boubaker J, et al. Chemical investigation of different extracts and essential oil from the tubers of (Tunisian) Cyperus rotundus. Correlation with their antiradical and antimutagenic properties. Ann Microbiol. 2007; 57:657-64. [DOI:10.1007/BF03175369]

[21] Priya Rani M, Padmakumari KP. HPTLC and reverse phase HPLC methods for the simultaneous quantification and in vitro screening of antioxidant potential of isolated sesquiterpenoids from the rhizomes of Cyperus rotundus. J Chromatogr B Analyt Technol Biomed Life Sci. 2012; 904:22-8. [DOI:10.1016/j.jchromb.2012.05.042] [PMID]

[22] Koduru S, Grierson DS, Van De Venter M, Afolayan AJ. Anticancer activity of steroid alkaloids isolated from Solanum aculeastrum. Pharm Biol. 2007; 45(8):613-8. [DOI:10.1080/13880200701538690]

[23] Andrews JM. Determination of minimum inhibitory concentrations. J Antimicrob Chemother. 2001; 48(Suppl 1):5-16. [DOI:10.1093/jac/48.suppl_1.5] [PMID]

[24] Anusha CS, Kumar BP, Sini H, Nevin KG. Antioxidant aerva lanata extract supresses proliferation and induce mitochondria mediated apoptosis in human hepatocelluar carcinoma cell line. J Exp Integr Med. 2016; 6(2):71-81. [Link]

[25] Gurst JE. NMR and the structure of D-glucose. J Chem Educ. 1991; 68(12):1003-4. [DOI:10.1021/ed068p1003]

[26] Coates J. Interpretation of infrared spectra: A practical approach. In: Meyers RA, editor. Encyclopedia of analytical chemistry: Applications, theory, and instrumentation. Hoboken: Wiley; 2011. [DOI:10.1002/9780470027318.a5606]

[27] Onche EU, Tukura BW, Bako SS. Nuclear magnetic resonance (NMR) analysis of D - (+) - glucose: A guide to spectrometric structural elucidation of sugars. J Appl Chem Biotechnol. 2013; 6(1):45-51. [DOI:10.9790/5736-0614551]

[28] Singh NK, Pandey BR, Verma P, Bhalla M, Gilca M. Phytopharmacotherapeutics of Cyperus rotundus Linn. (Motha): An overview. Indian J Nat Producs Resour. 2012; 3(4):467-76. [Link]

[29] Jahan N, Ur-Rahman K, Ali S, Asi MR. Phenolic acid and flavonol contents of gemmo-modified and native extracts of some indigenous medicinal plants. Pak J Bot. 2013; 45(5):1515-9. [Link]

[30] Zhou Z, Fu C. A new flavanone and other constituents from the rhizomes of Cyperus rotundus and their antioxidant activities. Chem Nat Comp. 2013; 48:963-5. [DOI:10.1007/s10600-013-0439-x]

[31] Chang CC, Yang MH, Wen HM, Chern JC. Estimation of total flavonoid content in propolis by two complementary colometric methods. J Food Drug Anal. 2002; 10(3):178-82. [DOI:10.38212/2224-6614.2748]

[32] Kandikattu HK, Rachitha P, Krupashree K, Jayashree GV, Abhishek V, Khanum F. LC-ESI-MS/MS analysis of total oligomeric flavonoid fraction of Cyperus rotundus and its antioxidant, macromolecule damage protective and antihemolytic effects. Pathophysiology. 2015; 22(4):165-73. [DOI:10.1016/j.pathophys.2015.07.001] [PMID]

[33] Kumar KH, Khanum F. Hydroalcoholic extract of cyperus rotundus ameliorates H2O2-induced human neuronal cell damage via its anti-oxidative and anti-apoptotic machinery. Cell Mol Neurobiol. 2013; 33(1):5-17. [DOI:10.1007/s10571-012-9865-8] [PMID]

[34] Bray F, Ferlay J, Soerjomataram I, Siegel RL, Torre LA, Jemal A. Global cancer statistics 2018: GLOBOCAN estimates of incidence and mortality worldwide for 36 cancers in 185 countries. CA Cancer J Clin. 2018; 68(6):394-424. [DOI:10.3322/caac.21492] [PMID]

[35] Tholl D. Biosynthesis and biological functions of terpenoids in plants. Adv Biochem Eng Biotechnol. 2015; 148:63-106. [DOI:10.1007/10_2014_295] [PMID]

[36] Maneerat W, Phakhodee W, Ritthiwigrom T, Cheenpracha S, Promgool T, Yossathera K, et al. Antibacterial carbazole alkaloids from clausena harmandiana twigs. Fitoterapia. 2012; 83(6):1110-4. [DOI:10.1016/j.fitote.2012.04.026] [PMID]

[37] Soumaya KJ, Zied G, Nouha N, Mounira K, Kamel G, Geneviève FD, et al. Evaluation of in vitro antioxidant and apoptotic activities of Cyperus rotundus. Asian Pac J Trop Med. 2014; 7(2):105-12. [DOI:10.1016/S1995-7645(14)60004-3] [PMID]

[38] Toné S, Sugimoto K, Tanda K, Suda T, Uehira K, Kanouchi H, et al. Three distinct stages of apoptotic nuclear condensation revealed by time-lapse imaging, biochemical and electron microscopy analysis of cell-free apoptosis. Exp Cell Res. 2007; 313(16):3635-44. [DOI:10.1016/j.yexcr.2007.06.018] [PMID] [PMCID]

[39] Goldar S, Khaniani MS, Derakhshan SM, Baradaran B. Molecular mechanisms of apoptosis and roles in cancer development and treatment. Asian Pac J Cancer Prev. 2015; 16(6):2129-44. [DOI:10.7314/APJCP.2015.16.6.2129] [PMID]

[40] Zhang H, Loveridge ST, Tenney K, Crews P. A new 3-alkylpyridine alkaloid from the marine sponge Haliclona sp. and its cytotoxic activity. Nat Prod Res. 2016; 30(11):1262-5. [DOI:10.1080/14786419.2015.1054826] [PMID] [PMCID]

This Page Intentionally Left Blank